Peer-reviewed version available at Materials 2017, 10, 176; doi:10.3390/ma10020176

Article

Fundamentals of the Behavior of Concrete Recycled with PET Additives through Its Porosity

J. Miguel Mendivil-Escalante [1], J. Manuel Gómez-Soberón [2,*], J. Luis Almaral-Sánchez [1] and F. Guadalupe Cabrera-Covarrubias [3]

[1] Faculty of Engineering Mochis, Autonomous University of Sinaloa, Fuente de Poseidón y Ángel Flores s/n, Col. Jiquilpan, Module B2, 81210 Los Mochis, Sinaloa, Mexico; josemiguelmendivil@hotmail.com (J.M.M.-E.); jalmaral@uas.edu.mx (J.L.A.-S.)

[2] Barcelona School of Building Construction, Polytechnic University of Catalonia, Av. Doctor Marañón 44-50, 08028 Barcelona, Spain

[3] Barcelona School of Civil Engineering, Polytechnic University of Catalonia, C. Jordi Girona 1-3, Building C2, 08034 Barcelona, Spain; guadalupe.cabrera04@gmail.com

* Correspondence: josemanuel.gomez@upc.edu; Tel.: +34-934-016-242

Abstract: In the field of construction, materials referred to as sustainable are currently undergoing a process of technological development. This study aims to contribute to the understanding of the behavior of the fundamental properties of concretes prepared with recycled coarse aggregates that incorporate in their matrix a polyethylene terephthalate-based additive in an attempt to reduce their high porosity. Techniques to measure the gas adsorption, water porosity and x-ray diffraction (XRD) were used to evaluate the effect of the additive on the physical, mechanical and microstructural properties of these concretes. Porosity reductions of up to 30.60% are achieved with the addition of 1, 3, 4, 5, 7 and 9% of the additive, defining a new state in the behavioral model of the additive (the overdosage point) in the concrete matrix; in addition, the porous network of these concretes and their correlation whit other physical and mechanical properties are also explained.

Keywords: PET[1] additives; recycled concrete; concrete porosity; polymeric resins; porosimetry of nitrogen (N_2) gas adsorption; acoustic resonance spectroscopy

1. Introduction

The current level of the technological development of concrete is focused on the optimization of its characteristics, components, mechanical properties and in particular in their durability. Parallel to this development, a new sustainable concept for concrete has emerged, known as recycled concrete (RC), which is produced by the mixture of natural stone aggregates and recycled coarse aggregates (RA_{coarse}) agglutinated using a cement paste [1-2]. This development was born out of the intention to satisfy the current need for the use of construction waste [3-4]. The foregoing has been tested in various countries across the practices aimed at the conservation of natural resources increasing of the useful lifespan of sanitary landfills, and thus avoiding the exploitation of non-renewable natural resources [5].

As an alternative for improving the properties of concrete and contributing to the sustainability of the environment, research is underway on the use of polyethylene terephthalate (PET) as a component of RC. This substance, via its transformation into an unsaturated polyester resin, could be used as an additive to improve the performance of RC [6]. This material is often found in plastic bottles, which have a wide variety of uses and, thus, is cause of huge amounts of waste [7]. In order that it is no longer considered waste, new sustainable applications for this can be developed, such as new polymer variants and textile applications, or as a possible densifier for concretes [8]. In general, the use of polymers in concretes began in the 1960s replacing fractions of the aggregates [9];

[1] PET: polyethylene terephthalate

Peer-reviewed version available at Materials 2017, 10, 176; doi:10.3390/ma10020176

nowadays, the evolution of the application of polymers in concretes has enabled the creation of a polymer-modified concrete (PMC), comprising conventional concrete mixed with a polymer resin [10], with the polymer used, in this case, being PET.

PMC is used in structural applications, pavement, wastewater pipes, repairs, and concrete surface coatings etc., providing sufficient durability levels in all applications [11-12] such as: the effects of the environment, chemical attacks, abrasion, or any other process [13]. On the other hand, the durability of a concrete tends to be linked to the process of water penetration, which transports the aggressive agent, and which, in turn, depends on the porosity of the concrete. This is a function of its pore structure and of its degree of connectivity, being the physical properties of its structure that finally establishes it [14] (capillary absorption, permeability and diffusion).

While it has been shown that the partial or total replacement of natural aggregates by recycled ones to produce an RC has a positive effect on environmental impact [15-16], this also causes an increase in the porosity of the concrete produced [17], which has repercussions in terms of durability. Therefore, it may be justifiable to propose the incorporation of an additive based in PET with the prevision of an increase in the densification of the paste that will reverse this effect, for which, the porosity study of these concretes is proposed in this research as a comparative instrument and an explanation of their behavior.

2. Materials and methods

2.1. Materials

The following processes were required to obtain the additive based in PET [18]. Firstly, the polymeric resin was synthesized from a recycled PET base taken from plastic bottles post-consumption, with the prior elimination of any other type of non-polymer material; their size was then reduced with a scissors-type cutting tool, the crushed material then washed in a 50% water and caustic soda solution to guarantee the elimination of impurities. The second phase of obtaining the additive involved a depolymerization (glycolysis) process undertaken in a reactor, using propylene glycol (50% of the weight of the PET) as a solvent, and zinc acetate (0.5% of the weight of the PET) as a catalyst. Finally, the process of synthesizing the resin was undertaken on the resulting product, which consisted in the addition of maleic anhydride and adipic acid at a molar ratio of 1.1:0.5:0.5, with the objective of obtaining the PET additive to be used in the research (recycled resin [RR]).

The recycled aggregate is taken from concrete used in hydraulic pavement and recovered from an uncontrolled landfill (original concrete [OC]), which was then subject to crushing (jaw) process, and sieved to obtain a size adequate to be used as aggregate for concrete. The basic properties of the OC are shown in Table 1.

Table 1. Properties of OC.

Property	Value
Absorption (%)	6.91
Density (g/cm^3)	2.36
Porosity (%)	17.87
Rebound index	28.15

ASTM C136 [19] was used to characterize the distribution of the particle size of the aggregates, obtaining the granulometric profiles from this test for both the natural fine aggregates (NA_{fine}) (Figure 1a) and natural coarse aggregates (NA_{coarse}), as well as the RA_{coarse} (Figure 1b). The NA_{fine} used was found to be within the ASTM C33 limits [20], while Figure 1b) shows both profiles exceeding the lower limit of between 12.7 and 25.4 mm, which indicates the existence of particle content of a larger size than that specified in the regulations. However, said characteristic is common in both aggregates as well as those habitually used in local pre-mixing plants. Therefore, it can be said that partial substitution will not affect the behavior of the concretes containing them – at least not due to the effect of the distribution of their particles).

Preprints (www.preprints.org) | NOT PEER-REVIEWED | Posted: 16 December 2016 doi:10.20944/preprints201612.0090.v1

Peer-reviewed version available at Materials 2017, 10, 176; doi:10.3390/ma10020176

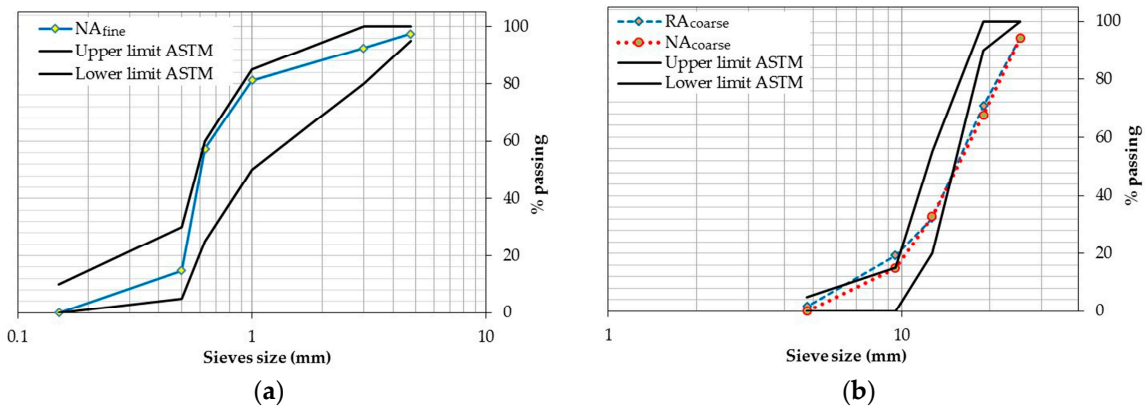

Figure 1. a) Granulometry of NA_{fine}; **b)** Granulometry of RA_{coarse} and NA_{coarse}.

With regard to the physical properties of the aggregates (ASTM C 642) [21], it should be noted (see Table 2) that, due to the singularity of the OC, the properties of the RA_{coarse} produced are seen to be affected. In particular, the high absorption of the OC causes in the RA_{coarse} of the order of five times more absorption than that obtained from the NA_{coarse}; however, it should be noted that both are in accordance with the regulations. To a lower extent, density reductions of up to 8% [22] are reported for the RA_{coarse} compared to the NA_{coarse}. In both cases (absorption and density), the variations detected are attributed to the porous nature of the old mortar adhering to RA_{coarse} [23].

Table 2. Properties of aggregates.

Property	RA_{coarse}	NA_{coarse}	NA_{fine}
Absorption (%)	6.27	1.19	1.88
Density (g/cm³)	2.38	2.56	2.59
Fineness modulus	-	-	2.53
Maximum size (mm)	19.05	19.05	4.76

2.2. Experiment

The preparation of the specimens of concrete modified with polymer and recycled aggregate (RPC) used a water/cement ratio (w/c) of 0.50 and 25% of NA_{coarse} substituted for RA_{coarse} in the samples, producing six types of mixtures whose sole modification was the level of RR content used (% added depending to the weight of the cement). Furthermore, as a control variable, one more mixture was prepared without the addition of RR. The values used for the dosages are shown in Table 3.

Table 3. Mixtures dosage.

Component	Classification of mixtures [1]						
	AF-0	AF-1	AF-3	AF-4	AF-5	AF-7	AF-9
Cement (Kg/m³)	350.00	350.00	350.00	350.00	350.00	350.00	350.00
Water (Kg/m³)	175.00	175.00	175.00	175.00	175.00	175.00	175.00
RA_{coarse} (Kg) (4.76 - 12.70 mm)	262.50	262.50	262.50	262.50	262.50	262.50	262.50
NA_{coarse} (Kg)(4.76 - 12.70 mm)	787.50	787.50	787.50	787.50	787.50	787.50	787.50
NA_{fine} (Kg) (1.00 - 4.76 mm)	700.00	700.00	700.00	700.00	700.00	700.00	700.00
RR (Kg)	-	3.50	10.50	14.00	17.50	24.50	31.50
w/c	0.5						

[1] AF = Adding Factor of RR, the second term provides the content thereof in the mixture.

The mixing process consisted in introducing the components into the mixer in the following sequential order: the cement content and the NA_{fine} (in a dry state) were introduced to the mixer for one minute at speed of mixing; the RA_{coarse} and NA_{coarse} were then added (both in a saturated surface-dry condition, achieved by immersion in water for 24 hours, and after evaporation of the excess [by extended and ventilation]) to this mixture, which was left in the moving mixer for one minute more until homogenization. Water was then added to the mixture, which was then left to stand for 30 seconds in order to saturate the NA_{fine} and begin hydrating the cement; finally, the mixing process was carried out for one minute, and in order to incorporate the RR into the mixture, an extra minute applied.

Three cubic (10 x 10 x 10 cm) and three prismatic (4 x 4 x 16 cm) specimens were prepared for each of the mixtures used in this study (ASTM C192) [24], which, 24 hours after molding, were demolded and then submerged in water until being submitted to testing (28 days of curing) at room temperature in the laboratory.

Standard ASTM C642 [21] was used for the characterization of the physical properties to be used in correlation with the porous network of the RPC, obtaining the absorption, apparent density and total water porosity for each sample. Table 4 presents the results.

Table 4. Physical properties of RPC.

Parameters	Classification of mixtures						
	AF-0	**AF-1**	**AF-3**	**AF-4**	**AF-5**	**AF-7**	**AF-9**
Bulk density (g/cm^3)	2.45	2.47	2.52	2.53	2.56	2.59	2.53
Pore volume (%)	12.02	11.26	10.92	10.63	10.21	10.03	10.31

For apparent density and generally terms, the use of the RR produces slight increases (up to 6%) compared to AF-0. Finally, in reference to the porosity of the samples, the highest value was presented by AF-0, with values gradually reducing as the RR factor was increased, until falling to the difference of 1.99% (when AF-7 is compared whit the control sample), to then increase again in AF-9.

The previous results can be attributed to the effect of the RR on the mixtures, conjectured from this behavior that the additive used can cause variations in the RPC matrix; therefore, the open porous network is initially obstructed following the introduction of the additive, which also produces an increase in density. Finally, it should be noted that the changes produced in a resistant and durable concrete present improvements in terms of the densification of the matrix.

The dynamic modulus of elasticity (Ed) was chosen as a mechanical property to be studied in the RPC, as it is one of the properties of resistance that best describe the behavior of concretes, further to being easy to obtain and non-destructive (ASTM C215) [25]. The acoustic resonance spectroscopy procedure is based on the detection of the frequencies generated by impact on the specimen, which are transmitted through the specimen and then captured by the sonic receiver (microphone). The system completed the process via the algorithm and the calculation of the frequencies, correlating mass, density and the propagation longitudinal elastic waves [26].

Table 5 presents the results obtained, from which it can be seen that the increase in RR content generates increases of 16-17% for the variables studied compared to the control sample. These results present a direct correlation with density, and, consequently, with an inverse relationship with the absorption parameter, which is attributed to the reduction in the porosity of concretes. In all cases, the variations in the behavior of the RPCs are related to the different levels of RR content.

Table 5. Dynamic modulus of elasticity.

Mixture	Ed (GPa)
AF-0	25.64
AF-1	26.68
AF-3	27.61
AF-4	28.24
AF-5	29.28
AF-7	29.87
AF-9	29.56

2.3. *Characterization of the porous network*

Gas (N_2) adsorption porosimetry was selected as a technique for characterizing the porosity of the RPCs in this study, as it provides sufficient resolution for the porosity in the zones known as micropores and mesopores (less than 2 and 50 nm, respectively) [27]; being these zones, where porosity increase is foresee by the presence of the mortar adhered in the RA_{coarse}, and likewise, feasible reduction by the use of RR.

This technique is used to determine the total volume of the porosity, in order to define pore distribution, and estipulate the specific surface of the porous materials. It has, as a general principle, the quantification of the molecules of a gas that are found to be attracted to the solid surface of a material, leading to the process known as gas adsorption, in contrast to the phenomena of gas absorption, in which the gas molecules do penetrate the solid.

In the case of gas adsorption, the complete test process includes two differential phases, the first of which is known as enrichment (positive adsorption or intrusion) and the second is known as emptying (negative adsorption or desorption). Both curves do not necessarily follow identical trajectories, which leads to different interpretations or explanations of the phenomena that they are characterizing.

The nitrogen (N_2) gas used is considered the best adsorptive for the analysis and determination of pore size, owing to the fact that the thickness of the multilayers is not sensitive to the different types of absorbents. This enables the isotherm used in the test to establish both the pore distribution and specific surface; this last, it is considered a measurement of the surface as a dimension, which, referring to a one-unit mass of the solid is taken as the specific surface area. The BET (Brunauer, Emmett, Teller) method was used to determine the number of adsorbed molecules that form a monolayer on the surface, in order to then relate this with the specific surface area of the solid in question, using the area occupied by a molecule [28].

When a porous solid is exposed to a pressurized gas, it begins to adsorb the gas, this phenomenon is evidenced by two determinations: an increase in the weight of the solid (determined on a bascule); and, by a drop in pressure inside the sealed test chamber. After a test time period has passed, the pressure is stabilized at a value the instant that the solid reaches its maximum weight. From the pressure drop onwards, with the volumes of both the sample and the test chamber established, the ideal gas law is used to determine the amount of gas adsorbed, which is related to the total pore volume [29].

Whit regard to the preparation of the samples studied, and as a requirement of the equipment used (Micromeritics, Tristar), the RPC specimens were manually crushing, selecting the representative particles that satisfy the criteria: a size smaller than 4 mm; and, a total volume until reaching the maximum allowed in the test (3.3 cm^3).

3. Results

The results of the analysis of the N_2 adsorption tests undertaken on the different study samples are presented below. Figure 2 details the distribution of the average pore radiuses at the adsorption

stage, with all the samples presenting average radiuses, which are mainly found within the mesopore range (1-25 nm), denoting that the possible structural changes in the matrices of these concretes should be studied in the paste [30]. Moreover, it should be noted that the porosity of samples AF-1 to AF-7 is reduced depending on the RR content when compared to the control sample AF-0. Similarly, AF-9 presents a significant reduction in porosity, although to in a lower rank than the other samples, thus placing it above them (effect of RR overdosage with an inflection point in the mesopores between the samples AF-7 and AF-9, Table 5).

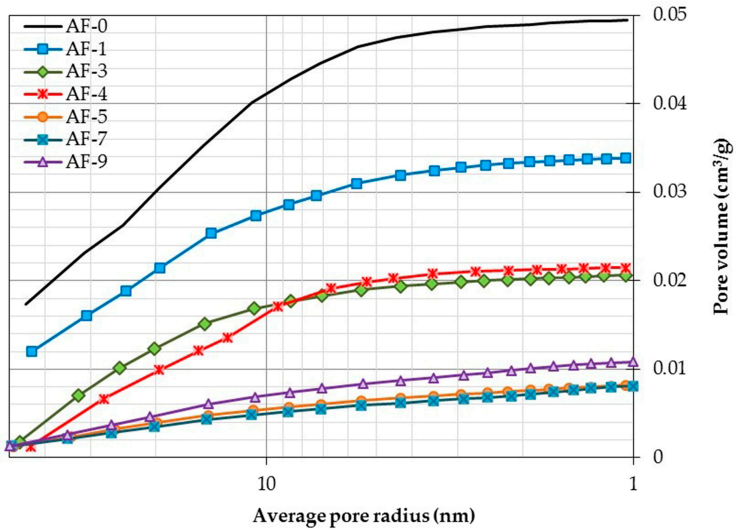

Figure 2. Distribution of pores by adsorption.

The RR dosage analysis denotes an inverse correlation between the pore radius reduction and RR dosage, thus causing mechanics improvements as those previously presented. This behavior is explained by the formation of what is known as the polymeric film of a RPC, which becomes thicker and more rigid with the increased of RR in the concrete, and, for which, exists a previous modeling [31].

In the specific case of AF-9, the tendencies indicated above do not appear to be valid, as evidenced by the fact the porosity does not continue to decrease as foreseen, instead increasing until reaching an increase of 2.8% (compared to AF-5 and AF-7, although still below AF-0). The above described indicates that a point of RR overdosage exists between content of 7 and 9%, causing a possible non-optimal dispersion of RR within the cementitious matrix, generating zones in which it agglomerates, and enabling the natural hydration process (continuous porosity) to occur. An RR overdosage increases the "packaging" capacity of cement particles, slowing (or even encapsulating whit blocking) the formation of the hydration products responsible for the formation, structure and porosity of the CH and CSH of a concrete [32], thus leading to a potential cementitious matrix that does not develop due to the blocking of its cement particles, and in this way is prevented from achieving optimal hydration.

In the constitutive modeling of RPC and taking as a model that proposed by Beeldens [31], the four simplified stages are as follows: Stage 1) The formation of the alkaline solution of pore by the initial hydration of the cement; Stage 2) Deposit of RR on the surface of the aggregates and the partial or total coating of some cement particles and, furthermore, the formation of a continuous film with preferential provision in the surface of the hydrates; Stage 3) Continuous hydration and formation of the polymeric film; and, Stage 4) Comprising the culmination of the final hydration process of the cement, consolidation of the continuous phase of the RR through the cementitious matrix, extraction of the excess water from the pore solution, restriction of the capillary pores, and the formation of bridges between the aggregates. The four stage described are valid for explaining the AF-1, AF-3, AF-4, AF-5 and AF-7 studied here; however, for the AF-9 mixture (overdosage), only the three first stages can be applied, requiring, in this new case (overdosage), the replacement of Stage 4 by a new stage

within the model for the hydration of a RPC, to which it has been called as Stage 4RR$_{exceeded}$ (see Figure 3). This last stage is also characterized by being the final phase of hydration and the consolidation of the continuous film of the RR, but also partial particular phases occur in this: part of the RR particles result in agglomerations of isolated products within the matrix, avoiding the formation of efficient bridging between the aggregates (unbound bridge); in addition also, the anhydrous cement particles can not develop their full crystallization because this it is inside the film formed by the coverage of the RR, thereby preventing an expected densification in the RPC (encapsulated particle).

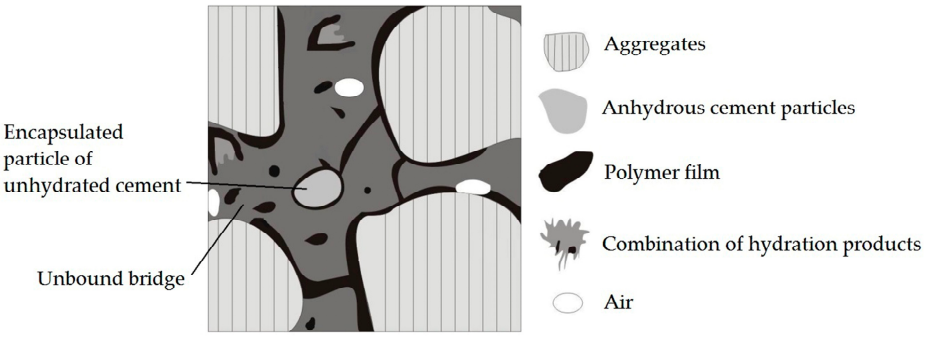

Figure 3. New Stage 4RR$_{exceeded}$ product of overdosage.

To corroborate the above, the formation of the principal products of hydration was determined for cases AF-5 and AF-7 through X-Ray Diffraction (XRD) (see Figure 4), in this, the calcium hydroxide (CH) (1) peaks can be appreciated, as well as the zones of increase in the formation of hydrated calcium silicates (CSH) (2). In both cases, the behavior described by the diffractograms relates to the detection of more defined peaks, which are clear and more intense in direct relation to the RR content, taking AF-0 as a reference. However, for case AF-9, the variations in the formation of products of hydration present tendencies of lower intensity peaks in both hydrates, with this thus indicating a loss of hydration capacity in the mixture caused by the effect of the RR overdosage.

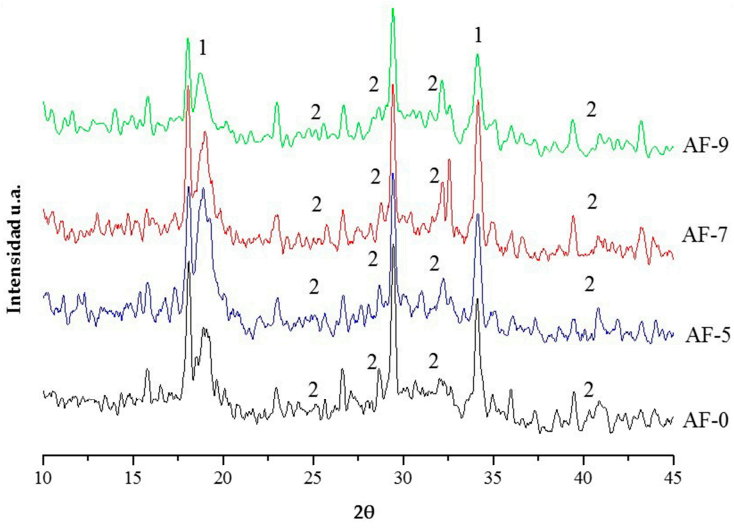

Figure 4. XRD of RPC. 1: CH; 2: CSH.

With regard to the quantity of adsorbed gas (total porosity), Table 6 indicates that the order of porosity increase in the samples studied is AF-7, AF-5, AF-4, AF-9, AF-3, AF-1 and AF-0 (the order expected according to prior studies), reaching a maximum difference of 21.27% between AF-7 whit respect AF-0.

As a constant characteristic of the distribution of radius size, all the samples present higher percentage sizes in the mesopore zone, reporting a variation in absolute terms of only 3.05, representing a significance to the order of 5% within these sizes. According to Figure 2, and

Peer-reviewed version available at Materials 2017, 10, 176; doi:10.3390/ma10020176

determining the greater absolute variation of pore size in the other two size zones, the macropore zone appears to be key to the variation in the behavior of the mixtures with the use of RR, reporting a 2.64% variation in the absolute value of these sizes. However, compared to the mesopore zone, this represents a significance of up to 7.33%.

Table 6. Pore size distribución.

Mixture	Total porosity (cm^3/g)	Macropores (> 25 nm)%	Mesopores (1 - 25 nm)%	Micropores (< 1 nm)%
AF-0	0.04954	38.34	59.62	2.04
AF-1	0.04900	33.38	64.94	1.68
AF-3	0.04800	38.34	59.62	2.04
AF-4	0.04667	34.03	63.39	2.58
AF-5	0.04600	32.44	65.21	2.35
AF-7	0.03900	38.51	59.51	1.98
AF-9	0.04700	39.51	58.37	2.12

The behavior of the specific BET surface is presented in Figure 5, which shows a notable decrease for AF-5, AF-7 and AF-9 compared to AF-0, which reaches, in general terms, a value of 71.83% for the group of variables studied. Technological alternatives that are able to facilitate this type of densification in concretes can only be attained under strict conditions for the design and posterior manipulation of dosage [33], or using unusual components that produce "special concretes" [34].

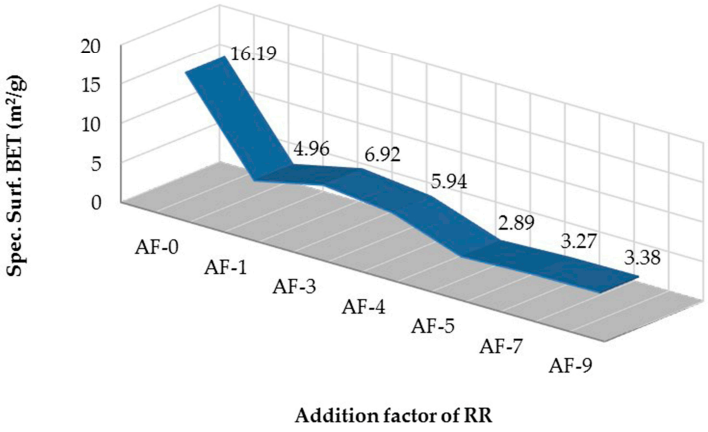

Figure 5. Specific surface (BET) of the different mixtures tested.

Within the isothermic curve (theoretical pore radius vs. volume of adsorbed N_2) three radius sizes of interest can be identified, which can be used to describe and understand the behavior of the test samples. Such radiuses are classified into three typologies: the known as the maximum radius, designation used to define the greatest radius value detected in the test; the medium radius that is statistically able to represent the radius value that corresponds to the half of the volume of the total adsorption of the test, localizing said value on the axis of the abscissa of the graph; and, finally, the critical radius of saturation, which refers to the size of the pore in which gas adsorption initiates a drastic decrease in the adsorbed volume (the end of the test process), and is identified by the change in slope of the curve, becoming a straight line with constant slope. For its determination, the first pore radius causing a change on the slope of the curve with an angle greater than 5° was chosen, taking 87.1° - 86.5° as a common range from all the samples for its possible identification, measured from the vertical axis as origin and with reference to the horizontal axis in an anti-clockwise direction.

For the first of the radiuses of interest (maximum radius), a correlation between these and the physical properties of the RPC was established, indicating that the porosity (to water) reaches a high determination factor (see Figure 6) for the adjustment of a straight line with a constant inverse slope (an increase in the maximum pore radius produces lower pore volumes). That which has attained a linear equation could denote the high correlation between both parameters, helping to explain the porous network of the RPC. However, a priori, it can be said that it appears that the change from lower radius maximum pores to ones with a larger radius reduces total porosity to water. This could be explained by the hypothesis that while RR causes the porosity of average or small radiuses to be sealed, it is not able to do this with large radius pores, which in turn, remain open and are able to contain a higher quantity of water absorbed in the RPC.

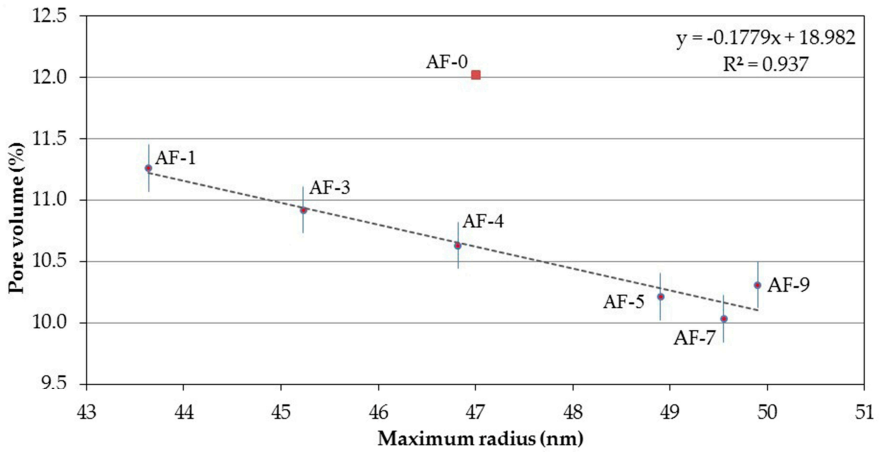

Figure 6. Maximum radius vs. Pore volume (to water).

In terms of the correlation indicated in Figure 7 for the maximum radius and Ed, the best determination factor attained was $R^2 = 0.9831$, with a linear curve fit. However, in contrast to the previous case, on this occasion, there is an ascending incremental relationship. The explanatory hypothesis for this is that the technique used in the determination of Ed is based on the measurement of the frequency of impact through the element, observing that when the RR causes the change in the maximum radius (small or medium) to large, the remaining porosity of the element is sealed or densified. Therefore, this generates more compact and continuous element that facilitate an improved passage and reception of the signal and, thus, higher Ed values.

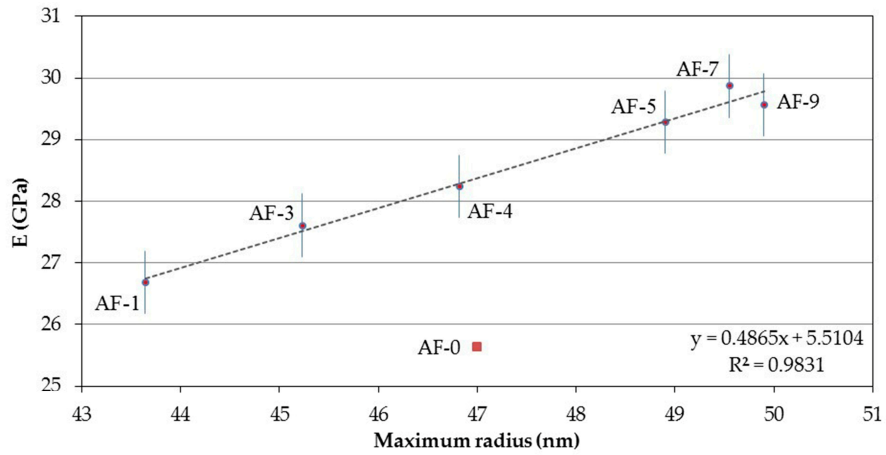

Figure 7. Maximum radius vs. Modulus of elasticity.

Relating the medium radius and total porosity (to water) obtains a straight line of fit with an ascending slope, which, in this case (due to its type of fit and direction), is one of the correlations between the porous network and physical properties of a concrete, that can be better and more simple

Preprints (www.preprints.org) | NOT PEER-REVIEWED | Posted: 16 December 2016 doi:10.20944/preprints201612.0090.v1

Peer-reviewed version available at Materials 2017, 10, 176; doi:10.3390/ma10020176

explained (see Figure 8). This is because the medium radius is a representative value of the entirety porosity of a concrete; increases in porosity to water are the natural result of medium radius increases.

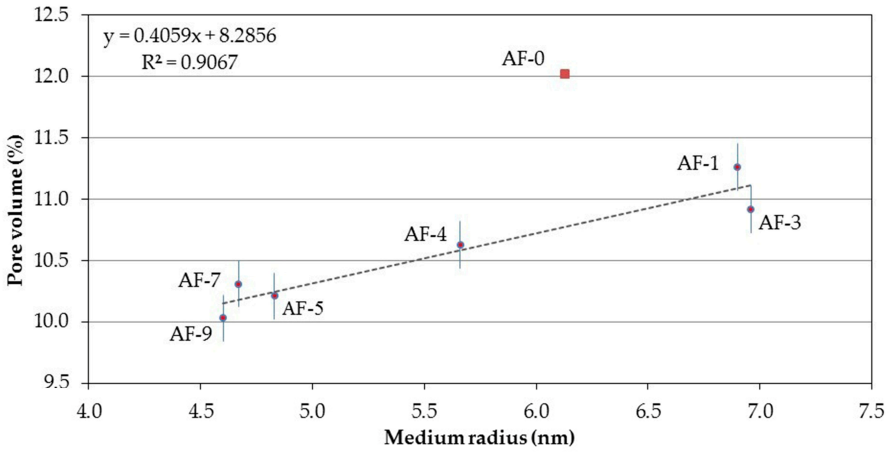

Figure 8. Medium radius vs. Pore volume.

With regard to the medium radius, it is feasible to establish a correlation between this and the corresponding Ed (Figure 9) using a linear regression with an inverse slope. The linear nature of the equation denotes a strong link between the calibration parameter (medium radius) and the independent variable Ed. This property is therefore better explained for the RPC (with the medium radius) than with the maximum radius. This reasoning could be due to the origin or nature of the medium radius parameter (pore that is the equivalent to the half of the volume of porosity recorded in the adsorption of N_2 test); which is, thus, a clearly representative parameter for all the porosity present in the RPC, and, therefore, has a direct correlation expressed in a linear equation.

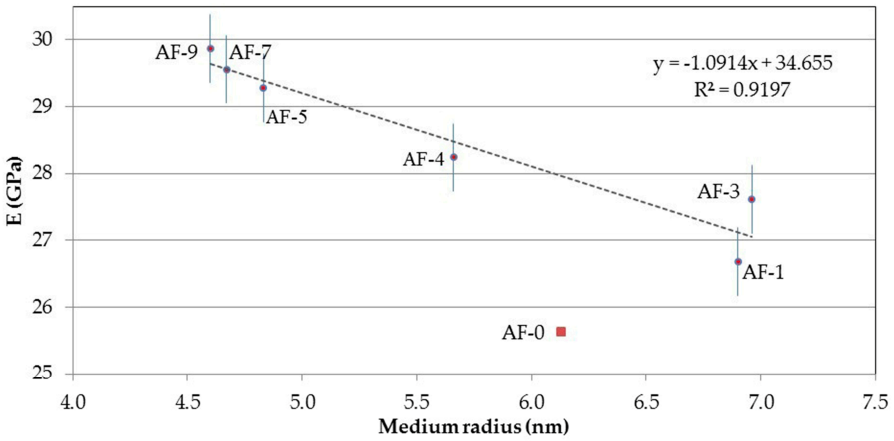

Figure 9. Medium radius vs. Modulus of elasticity.

Using that defined as the critical radius of saturation (start zone in the change in slope that moves from a curvature to an asymptotic straight line in the graph of average pore radius [nm] vs. intruded porosity [cm^3/g], which denotes the start of the saturation of pores by N_2), and correlated with Ed (Figure 10), is obtained a linear fit with an ascending slope (similar for the case with the medium radius and pore volume). Taking into account the fact that the slope in this case is more pronounced than that in the medium radius (implying faster changes or an accelerated variation of correlation), the interpretation of this term –in similar situations– should be selected as the one of most interest as a parameter that allows to explain or define in a more adequate way the mechanical phenomenon of the Ed of the RPC (greater possible path of the line).

Peer-reviewed version available at Materials 2017, 10, 176; doi:10.3390/ma10020176

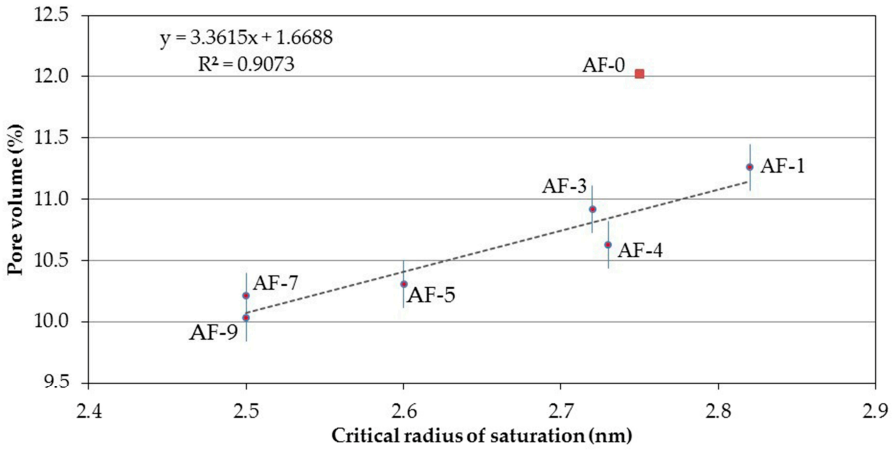

Figure 10. Critical radius of saturation vs. Pore volume.

The relationship between the porosity obtained via the adsorption of N_2 and the total porosity to water (see Figure 11) reported a very high significance in this research, which validates both techniques as comparable in terms of their capacity to characterize the porous structures of the RPC. On the other hand, of the different correlations previously presented that try to explain the porosity to the water of the PRC, this one is of quadratic polynomial type, interpreting this as that it is necessary to consider some other variable for the explanation of the phenomenon (not established in this research).

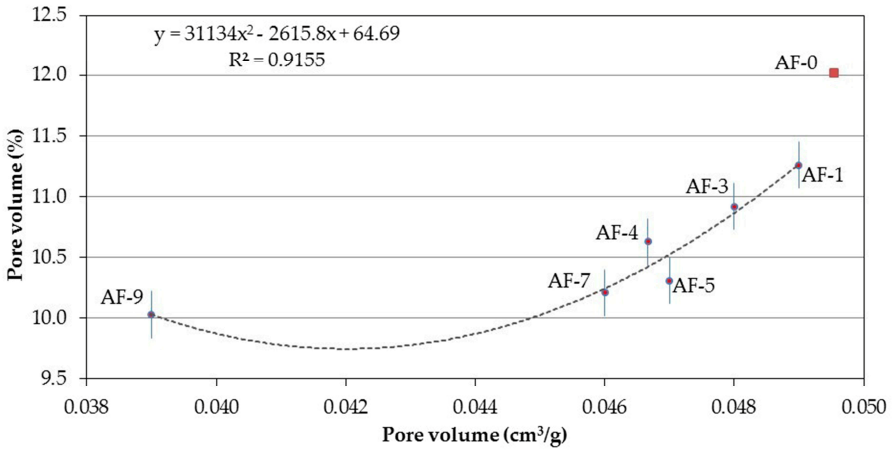

Figure 11. Pore volume (N_2) vs. Pore volume (to water).

Relating the N_2 pore volume to the density (see **Figure 12**) are obtained as best fit to an equation of the decreasing polynomial type, which corroborates that the reduction in total porosity improves the density results, with a tendency to increase this parameter due to the nature of the test itself.

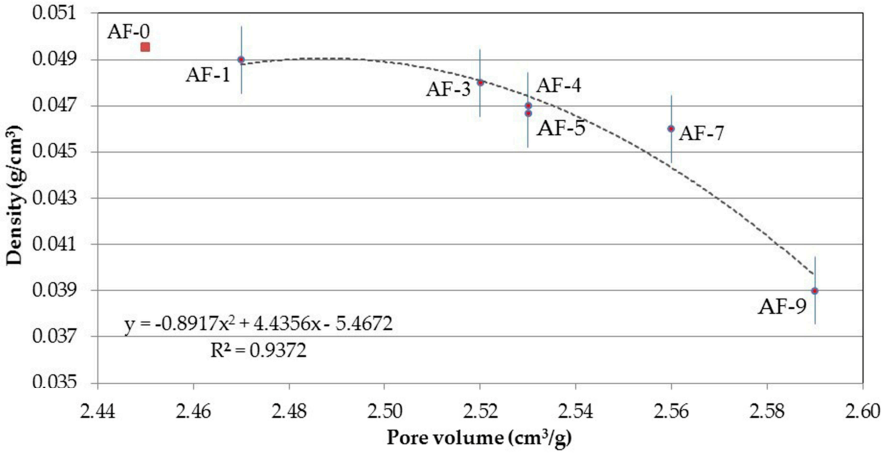

Figure 12. Pore volume vs. Density.

4. Conclusions

The study of the physical, mechanical and microstructural properties of RPCs has enabled the description of their behavior, which presents improvements through the use of percentages of RR additives comprising between 1 and 9%. Among the different properties studied, the porosity of the resulting matrix becomes one of the most favorable microstructural improvements obtained, achieving reductions of up to 16.55% less than the control specimen, while, for water absorption, values of up to 22.00% less were obtained. For the case of the dynamic modulus of elasticity, it is possible to obtain improvements of 16.50%.

The reduction in the porosity of the RPC is attributed to the formation of a cementitious matrix impregnated by a polymeric network, which is constituted among the bridging bound of the RR particles. These bridging bound are positioned with preferential orientation in order to bond with the aggregates, thus leading to the physical obstruction of the continuous porosity used for the conduction of fluids.

It is verified that RC considered as porous can mitigate this problem if they are designed using the additive RR, allowing in this way that the use of RA_{coarse} is equivalent to NA_{coarse} and thus achieving environmental improvements.

An inflection in the favorable behavior of its use has been found with the addition of the RR between 7 to 9%, this overdosage that causes the improvements detected in previous dosages to be reduced on using RR in proportions higher than 7%. This notwithstanding, for the 9% RR content studied here, the properties of these variables present improvements compared to the control sample (although below those recorded for lower RR content).

This overdosage is due to the agglomeration of RR particles that do not linked completely, obstructing of the pore sealing bridges, which thus remain isolated while also coating the cement hydrates and the particles of the aggregates that are encapsulated (loss of the reactive capacity for hydration contrasted by XRD). This new stage was designated Stage $4RR_{exceeded}$, which describes a new alternative for the behavior of overdosage in the use of RR based on previous studies.

The total porosity to water and the porosity by adsorption of N_2 are techniques that reliably express the correlations between the results and other properties that describe the behavior of the RPC mixtures studied. Among these correlations, this study has also verified, through ascending linear correlation, the best affinity with the results obtained. Finally, the parameter for the medium radius (obtained for the adsorption of N_2) enables the precise description and correlation established between the porous network of the RPC studied here, and the properties for Ed and the pore volume (to water); thus allowing them to explain in part their behavior.

Acknowledgments: The authors thank CONACYT for its doctoral scholarship program, the School of Engineering Mochis-UAS and the Barcelona School of Building Construction -UPC.

Author Contributions: J. Miguel Mendivil-Escalante (B, C, D), J. Manuel Gómez-Soberón (A, B, C, D, F), J. Luis Almaral-Sánchez (B, E, F), Guadalupe Cabrera-Covarrubias (B, D). Type of contribution: A - Research concept

and design. B - Collection and/or assembly of data. C - Data analysis and interpretation. D - Writing the article. E - Critical revision of the article. F - Final approval of article.

Conflicts of Interest: The authors declare no conflict of interest.

References

1. Castro, P.; Castillo, R.; Carpio, J.J. *Corrosión en estructuras de concreto armado. Teoría, inspección, diagnóstico, vida útil y reparaciones*, 2nd ed.: Instituto Mexicano del Cemento y del Concreto IMCYC, México, 2001.
2. Pomeroy, C.D. Concrete properties. *Phys. Bull.* **1972**, *23*, 657–658, DOI: 10.1088/0031-9112/23/11/015.
3. Sabet, D.B.; Lim, T.Y.D.; Teng, S. Ultra durable concrete for sustainable construction. *Adv. Mater. Res.* **2012**, *368–373*, 553–556. DOI: 10.4028/www.scientific.net/AMR.368-373.553.
4. Huda, S.B.; Alam, M.S. Mechanical behavior of three generations of 100% repeated recycled coarse aggregate concrete. *Constr. Build. Mater.* **2014**, *65*, 574–582, DOI: 10.1016/j.conbuildmat.2014.05.010.
5. Quin, Y.J.; Li, L.; Yibulayin, A.; Zhang, G.T. Experimental study on the fundamental characteristics of different parent recycled concrete fine aggregates. *Appl. Mech. Mater.* **2013**, *368–370*, 1080–1085, DOI: 10.4028/www.scientific.net/AMM.368-370.1080.
6. Guerra, T.K.; Proszek, G.J. Polymer concrete with recycled PET: The influence of the addition of industrial waste on flammability. *Constr. Build. Mater.* **2012**, *40*, 378–389, DOI: 10.1016/j.conbuildmat.2012.09.049.
7. Mohammad, K.; Amir, H.H.; Yahya, S.; Khadijeh, S.; Abolfazl, G. Chemical recycling of PET wastes with different catalyst. *Int. J. Polym. Sci.* **2015**, *2015*, 1–11, DOI: 10.1155/2015/124524.
8. Byung-Wan, J.; Seung-Kook, P.; Jong-Chil, P. Mechanical properties of polyester polymer concrete using recycled polyethylene terephthalate. *ACI Struct. J.* **2006**, *103*, 219-225, Available online: http://search.proquest.com/openview/3d6cb44832c2c606c90e6401ffd07616/1?pq-origsite=gscholar (accessed on 20 June 2014).
9. Jamshidi, M. A comparative study on physical/mechanical of polymer concrete and portland cement concrete. *Asian J. Civ. Eng.* **2010**, *11*, 421-432, Available online: http://www.sid.ir/en/VEWSSID/J_pdf/103820100402.pdf. (accessed on 4 July 2014).
10. Fowler, D.W. Polymers in concrete: a vision for the 21st century. *Cem. Concr. Compos.* **1999**, *21*, 449-452, DOI: 10.1016/S0958-9465(99)00032-3.
11. Garas, V.Y.; Vipulanandan, C. Review of Polymer Concrete Properties. *Dep. Civ. Environ. Eng.* **2003**, 1-3, Available onlines: http://www2.egr.uh.edu/~civeb1/CIGMAT/03_poster/11.pdf. (accessed on 10 August 2013).
12. Shivani, R.B.; Yuvraj, M.G. Polymer-modified concrete. *Int. J. Res. Eng. Technol.* **2015**, *4*, 845–848, DOI: 10.15623/ijret.2015.0404146.
13. Yueshun, C.; Jun, W.; Xiaolong, Z. Description of concrete durability damage process. Wuhan Univ. J. Nat. Sci. **2006**, *11*, 653–656, DOI: 10.1007/BF02836683.
14. Cheng, P.; Chen, X.F.; Wu, L. Research on Ordinary Concrete. *Durab. Appl. Mech. Mater.* **2014**, *584–586*, 1318–1321, DOI: 10.4028/www.scientific.net/AMM.584-586.1318.
15. Saeed, A.; Hammons, M.I. Use of recycled concrete as unbound base aggregate in airfield and highway pavements to enhance sustainability. Proceedings of the Airfield and Highway Pavements Conference, Bellevue, Washington, October 15-18; American Society of Civil Engineers, 2008, 497–508. DOI: 10.1061/41005(329)43.
16. Ramadan, S.F.; Solikin, M.; Ir.sriSunarjono Effect of recycled coarse aggregate on concrete properties. *Int. J. Innov. Res. Sci. Eng. Technol.* **2015**, *4*, 19060–19068, DOI: 10.15680/IJIRSET.2015.0401084.
17. Gómez-Soberón, J.M.V. Porosity of recycled concrete with substitution of recycled concrete aggregate: An experimental study. *Cem. Concr. Res.* **2002** , *32*, 1301–1311, DOI: 10.1016/S0008-8846(02)00795-0.
18. Mendivil-escalante, J.M.; Almaral-sánchez, J.L.; Gómez-soberón, J.M.; Arredondo-rea, S.P.; Corral-higuera, R.; Castro-beltrán, A.; Cabrera-Covarrubias, F.G. New concrete additive by chemical recycling of PET. *Adv. Sci. Technol. Res. J. 8*, 1–5, 2014, DOI: 10.12913/22998624.1120307.
19. *Standard test method for sieve analysis of fine and coarse aggregate;* ASTM C136-96; American Society for Testing and Materials: West Conshohocken, PA., 1996.
20. *Standard specification for concrete aggregates*; ASTM C33/C33-11; American Society for Testing and Materials: West Conshohocken, PA., 2011.
21. *Standard test method for density, absortion and voids in hardened concrete;* ASTM C642-06; American Society for Testing and Materials: West Conshohocken, PA., 2006.

22. González-Fonteboa B.; Martínez-Abella F.; Carro-López D.; Seara-Paz, S. Stress-strain relationship in axial compression for concrete using recycled saturated coarse aggregate. *Constr. Build. Mater.* **2011**, *25*, 2335–2342, DOI: 10.1016/j.conbuildmat.2010.11.031.
23. Chakradhara, R.M.; Bhattacharyya S.K.; Barai, S.V. Influence of field recycled coarse aggregate on properties of concrete. *Mater. Struct.* **2011**, *44*, 205–220, DOI: 10.1617/s11527-010-9620-x.
24. *Standard practice for making and curing concrete test specimens in the laboratory;* ASTM C192/C192M-98; American Society for Testing and Materials: West Conshohocken, PA., 1998.
25. *Standard test method for fundamental transverse, longitudinal, and torsional resonant frequencies of concrete specimens;* ASTM C215-08; American Society for Testing and Materials: West Conshohocken, PA., 2008.
26. Chen, J.; Jayapalan, A.R.; Kim, J.Y.; Kurtis, K.E.; Jacobs, L.J. Rapid evaluation of alkali-silica reactivity of aggregates using a nonlinear resonance spectroscopy technique. *Cem. Concr. Res.* **2010**, *40*, 914–923, DOI: 10.1016/j.cemconres.2010.01.003.
27. Gómez-Soberón, J. Relationship between Gas Adsorption and the Shrinkage and Creep of Recycled Aggregate Concrete. *Cem. Concr. Aggregates*. **2002**, *32*, 1301–1311, DOI: 10.1520/CCA10442J.
28. Campos, E.R.; Barrios, V.I.; González, L.A.M. *Caracterización petrofísica de las formaciones geológicas de la antiforma de Arroyal (Aguilar del Campoó) como posibles rocas de almacén y sello en la planta de desarrollo tecnológico de almacenamiento geológico de CO_2 (Hontomín-Burgos);* Madrid Ciemat 2011, España; pp. 120-122.
29. Vidick, B. Specific surface area determination by gas adsorption: influence of the adsorbate. *Cem. Concr. Res.* **1987**, *17*, 845–847, DOI: 10.1016/0008-8846(87)90047-0.
30. Chen, Z.P.; Wang, N.; Zhang, S.Q.; Zheng, S.F. Experimental study on basic behavior of recycled fine aggregate mortar. *Adv. Mater. Res.* **2011**, *168–170*, 1680–1685, DOI: 10.4028/www.scientific.net/AMR.168-170.1680.
31. Beeldens, A.; Gemert, D.; Schorn, H.; Ohama, Y.; Czarnecki, L. From microstructure to macrostructure: an integrated model of structure formation in polymer-modified concrete. *Mater. Struct.*, **2005**, *38*, 601–607, DOI: 10.1007/BF02481591.
32. Van, G.D.; Beeldens, A. Evolution in modeling cement hydration and polymer hardening in polymer-cement concrete. *Adv. Mater. Res.* **2013**, *687*, 291–297, DOI: 10.4028/www.scientific.net/AMR.687.291.
33. Kumbhar, P.D.; Murnal, P.B. Assessment of suitability of existing mix design methods of normal concrete for designing high performance concrete mixes. *Int. J. Civ. Struct. Eng.* **2012**, *3*, 158–167, Available online: http://connection.ebscohost.com/c/articles/89095598/assessment-suitability-existing-mix-design-methods-normal-concrete-designing-high-performance-concrete-mixes (accessed on 14 January 2015).
34. Piovezam, I.A.R.; Meleiro, L.P.; Isa, M.M. Compressive strength of the self-compacting concrete: Influence of the puzzolanic activity of the calcareous and basalt. *Cienc. y Eng. Sci. Eng. J.* **2006**, *15*, 95–100, Available online: http://www.seer.ufu.br/index.php/cieng/article/viewFile/536/496 (accessed on 18 December 2014).